

In Situ SEM/EBSD analysis of fatigue crack propagation behavior of a super duplex stainless steel

Guocai Chai^{1, a*}, Ru Lin Peng^{2, b}, Karel Slamecka^{3, c} and Sten Johansson^{2, d}

¹Sandvik Materials Technology, R&D center, 811 81 Sandviken, Sweden

²Linköping University, Department of Mechanical Engineering, SE 581 83 Linköping, Sweden

³Brno University of Technology, Czech Republic

^{a*}guocai.chai@sandvik.com, ^bRu.Peng@liu.se, ^cslamecka@fmc.vutbr.cz, ^dstejo@ikp.liu.se.

Keywords: Fatigue crack propagation, Fatigue crack branching, fatigue crack deflection, fatigue closure, EBSD analysis, Duplex stainless steels.

Abstract.

Fatigue crack branching and deflection behaviour in an UNS S32750 (SAF 2507) duplex stainless steel has been investigated using an In-situ SEM/EBSD fatigue test and a conventional da/dN methodology. Occurrence of crack branching results mainly from the extrusions and intrusions of slip bands developed in the grains. The number of crack branches formed depends strongly on the loading condition and the microstructure of the material. The in-situ observation confirms that the formation of crack branches can significantly reduce the crack propagation rate that leads to crack growth retardation in the main mode I crack path. The crack branches formed are usually not ideal. They can propagate almost transversely to the main crack direction with a mode II stress intensity factor, SIF, and a rate that is much higher than that of the main crack.

Crack deflection occurs mainly at the phase boundaries. A high crack deflection can also lead to a crack growth retardation. The high crack deflection and branching behaviour leads to a high fatigue threshold value of the material investigated since they have caused high crack growth retardation and high crack closure.

Introduction

It is known that fatigue crack propagation behaviour is influenced by loading conditions, microstructures in the material and environment. Fatigue cracking can significantly deviate from the propagation directions that should be perpendicular to the main stresses in mode I. This may lead to the formation of crack deflection, kinking or branching [1, 2], and consequently cause significant retardation or even arrest of the subsequent crack propagation by reducing crack driving force [2, 3]. This crack tip stress shielding can therefore enhance crack growth resistance.

Although it is very difficult to analyse propagation behaviour of branched cracks, several analytical solutions have been developed to predict the propagation path of a branched crack and to calculate the mode I and II stress intensity factors. They confirm that the formation of fatigue crack branches reduce the stress intensity factors and therefore the crack propagation rate [3, 4]. They also predict that a shorter branch will arrest and a longer branch will return to the pre-overload propagation [3]. These discussions were mainly focused on the overloading conditions. Most direct observations of fatigue crack branching behaviour have been made using light optical microscopes (LOM) or scanning electron microscopes (SEM). Recently, several in-situ SEM and atomic force microscope (AFM) studies on the fatigue branching behaviour have been performed [5, 6]. In these researches, fatigue crack branching behaviour and subsequent fatigue crack retardation were observed [5]. With in-situ AFM, the microscopic crack branching behaviour can be investigated [6]. However, these

studies can not identify the slip systems that start crack branching. No information on the influence of stress intensity factor, SIF, on the fatigue crack branching behaviour has been reported.

Modern dual phase or multi phase alloys exhibiting a good combination of high strength and high ductility are widely used as structural materials. These alloys also display remarkable fatigue properties. The fatigue threshold values of ferritic-martensitic duplex steels can range up to 20 MPa.m^{1/2}, which is much higher than the threshold range of single phase alloys [7]. The high thresholds of multi phase alloys are considered to be attributed to crack deflection and branching, which cause unusually high long crack propagation resistance [7, 8]. In the present study, the fatigue crack deflection and crack branching behaviour will be investigated for an austenitic-ferritic duplex stainless steel using a newly developed in-situ SEM/EBSD fatigue test and a conventional da/dN method. The fatigue crack branching behaviour, the influence of stress intensity factor and crack branching mechanism will be focused. The slip systems for crack branching will be identified.

Experimental procedure

The material used was a hot rolled bar made of the austenitic ferritic duplex stainless steel SAF 2507 (equivalent to UNS S32750) with a diameter of 80mm (AD) and a nominal chemical composition (in wt%): 0.03% C, 80% Si, 1.2% Mn, 25% Cr, 7% Ni, 4% Mo, 0,3%N and Fe. The tensile properties in the rolling direction are shown in Table 1.

Table 1 Tensile properties of SAF 2507 bar material in rolling direction

Temperature [°C]	σ_{YS} [MPa]	σ_{TS} [MPa]	Elongation [%]
20	625	820	41.7

Fatigue crack growth (FCG) rate tests were performed using 18 mm thick compact C(T) specimens with TS orientation in an MTS servo-hydraulic machine (50kN) equipped with Instron 8500 + digital electronics, and controlled by the Fast Track Program-da/dN. The main tests were performed using K-gradient constant value of $C_g = -0.1 \text{ mm}^{-1}$ in air at RT. The mean stress ratio R is 0.1 and the frequency is 10 Hz. The fatigue crack paths and mechanisms were investigated using SEM and LOM. The chemical compositions of each phase were analyzed by energy disperse spectrometry (EDS). Evaluation of fatigue crack branching was done by analysing high-resolution bitmap images acquired at magnification 1000× by means of the LOM. Digitalized images were printed out and the crack path was traced and highlighted on the printouts with the help of the edge-filtering computer algorithms applied to the original bitmap files. The number of short branches together with the origin of their initiation (within the ferritic grain, within the austenitic grain, at the ferrite-austenite grain boundary) was assessed.

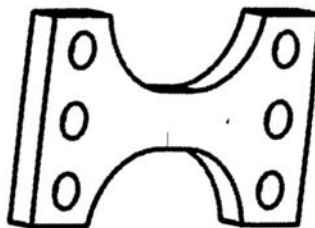


Fig. 1 The geometry of the tensile specimen for in-situ SEM/EBSD examination.

For in-situ SEM/EBSD experiments, a small specimen with a thickness of 2.5 mm and width of 5 mm was machined from a bending fatigue pre-cracked specimen with the crack at the mid-length of the gauge section. The geometry of the specimen is shown in Fig. 1. The length of the crack is 1.18 mm. Both sides of the specimen were ground and polished to remove the effect of machining. The side on which the EBSD studies were going to be performed was carefully prepared, following a procedure which always assures the removal of possible plastic deformation by the previous step. The final thickness at the cross-section is 1.513 mm.

The specimen was mounted on a Gatan microtester which was then inserted into the sample chamber of a Hitachi SU-70 scanning electron microscope. With the build-in pre-tilting fixture the carefully prepared surface of the specimen was in 20° tilt with respect to the incident electron beam. The EBSD detector and Channel 5 software from the Oxford Instrument were used for the in-situ EBSP mapping.

Tests with a peak load varying from 1800 N to 2800 N was carried out first to find a suitable growth rate which allows the in-situ experiment to be performed within a reasonable time frame. Finally, it was decided for a cyclic load between 2800 and 280 N (R=0.1), which induced, at the cross-section containing the crack, a maximum stress of 485 MPa and a minimum stress of 48.5 MPa. Loading was controlled via extension, with a fixed speed of 0.5 mm /min. A load cycle took about 80 seconds. The fatigue test was stopped after loading to different number of cycles for imaging by SEM or EBSP.

Results and discussion

Table 2 shows a summary of the testing results from a conventional fatigue propagation test for SAF 2507 bar material. The constants of the Paris law, C_m and n , were evaluated. $\Delta K_{cl,th}$ and $\Delta K_{eff,th}$, are also compared. This material shows very high closure threshold, $\Delta K_{cl,th}$, which are even higher than the effective thresholds, $\Delta K_{eff,th}$. The thresholds evaluated by analyzing the load versus crack opening displacement (COD) curves (sum of $\Delta K_{cl,th}$ and $\Delta K_{eff,th}$) are comparable to those determined from the da/dN vs ΔK curves, $\Delta K_{th,exp}$.

Table 2 Paris law's constants and threshold values

C_m (mm/cycle)	n	$\Delta K_{th,exp}$ (MPa√m)	$\Delta K_{cl,th}$ (MPa√m)	$\Delta K_{eff,th}$ (MPa√m)	$\Delta K_{cl,th} + \Delta K_{eff,th}$ (MPa√m)
5.35×10^{-10}	3.52	8.64	5,35	3,90	9,25

Fig. 2 shows a fatigue crack propagation profile for a conventional fatigue propagation test for SAF 2507 bar material at RT. The arrows indicate where a crack branching appears. It can be seen that the crack path is not straight and consists of numbers of crack deflections and crack branches. Fig. 3 shows some typical fatigue crack deflection behavior (Fig. 3a) and fatigue crack branching behavior (Fig. 3b). Fatigue crack deflection has occurred mainly at the phase boundaries. The propagating crack changes its direction when it meets or leaves the phase boundary. This crack deflection can lead to the formation of micro bands with “hills” or “valleys” on the fracture surface. They look like zones of different ΔK in one single phase alloy or as the crack arrested zones. Each band belongs to the one single phase. This has led to a high surface roughness induced crack closure, and consequently a high resistance to the propagation of long fatigue cracks in the near-threshold region [8].

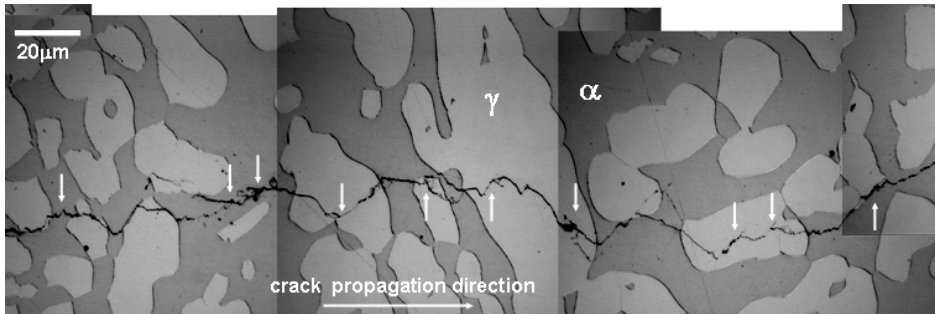


Fig. 2 Fatigue crack path from a conventional fatigue propagation test for SAF 2507 bar material. The arrows indicate where a crack branching appears. γ is the austenitic phase and α is the ferritic phase.

As shown in Fig. 3b, fatigue crack branching can occur in both ferritic and austenitic phases, but can also be observed at phase boundaries. Most of the branches are not ideal. The angle between two branches (2θ) varies greatly. Some of them are close to 180° . There are mainly two types of branching events: (i) ‘short branches’ with the length $l \leq 15 \mu\text{m}$ and (ii) long branches with the length $l > 30 \mu\text{m}$. Only a few cracks ceased to grow at an intermediate length $15 \mu\text{m} \leq l \leq 30 \mu\text{m}$.

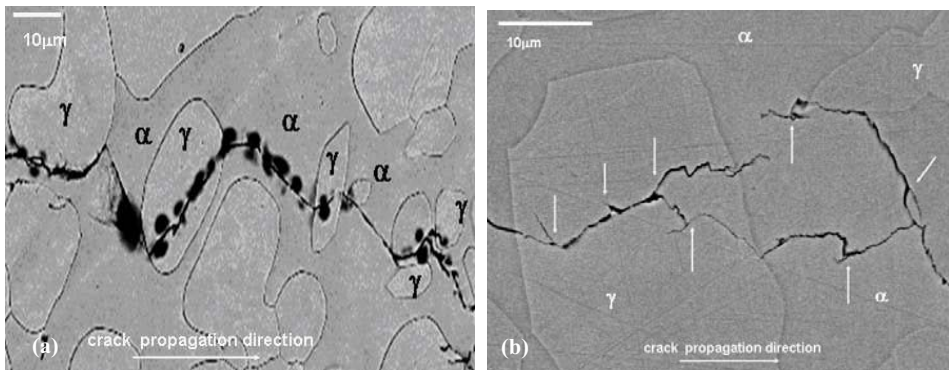


Fig. 3 (a). Fatigue crack deflection behavior and (b). Fatigue crack branching behavior in SAF 2507 bar material. The arrows indicate where a crack branching appears. γ is the austenitic phase and α is the ferritic phase.

It was observed that the occurrence of fatigue crack branching depends on the loading condition and the microstructure of the material. As shown in Fig. 4, the number of crack branches increase with increasing applied stress intensity factor ΔK . Near the fatigue crack threshold regime, the probability for the formation of fatigue crack branch has greatly reduced. Fig. 4 clearly shows that fatigue crack branching occurs mainly inside grains. It seems that the probability of the formation of fatigue crack branch is higher in the austenitic phase than in the ferritic phase. This may be due to the fact of the heterogeneous plastic deformation in this alloy [9]. The cyclic plastic deformation occurs first in the austenitic phase since it is the soft phase in the beginning [9]. This indicates that the formation of fatigue crack branches results from the cyclic damage due to the formation of slip bands. This was confirmed in reference [6] and the present EBSD work. The constraint of slip deformation due to the cyclic strain hardening is mainly responsible for crack branching [6].

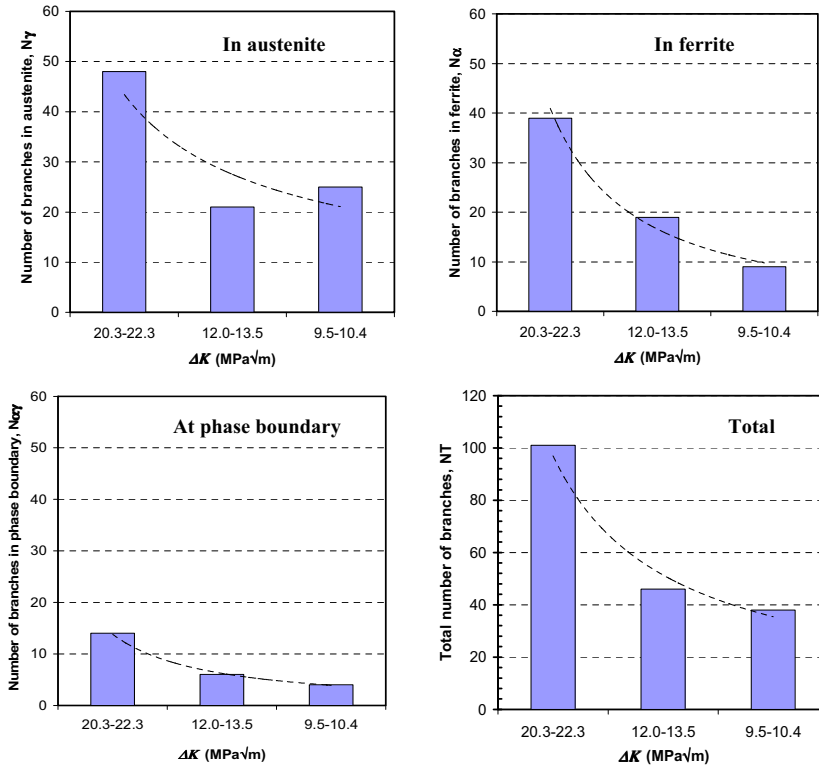


Fig. 4 Influence of load condition and microstructure on the formation of fatigue crack branching.

In the in-situ fatigue test, a very thin film was observed on the specimen surface, which was suspected to be Cr-oxide formed likely after the specimen preparation and before the in-situ fatigue test. The film cracked and delaminated where the crack propagated and thus prevent a close observation in certain regions. Nevertheless, much useful information has been obtained regarding the crack growth behavior, which are presented and discussed below.

The in-situ fatigue test was terminated after reaching 5100 cycle. The specimen was unloaded and the surface was cleaned with replica and acetone. Fig. 5a is a backscatter electron image, which reveals the crack geometry. Both crack deflection and branching are obvious. The first one appears at about 500 cycles (A) and the second one at about 3800 cycles (B), while the significant deflection is marked by 980 cycles (C). Fig. 5b is an EBSD image of the region taken before the fatigue crack passed through, in which the microstructure of the duplex stainless steel is shown. The high angle grain boundaries, plotted in thin black lines, are defined as larger than 10 degrees. A microstructure with fine austenitic grains (red) distributed in a matrix of relatively large ferritic grains (blue) is clearly shown. Furthermore, the distribution of austenite is not homogenous. In certain regions, bands containing mainly austenitic grains are observed.

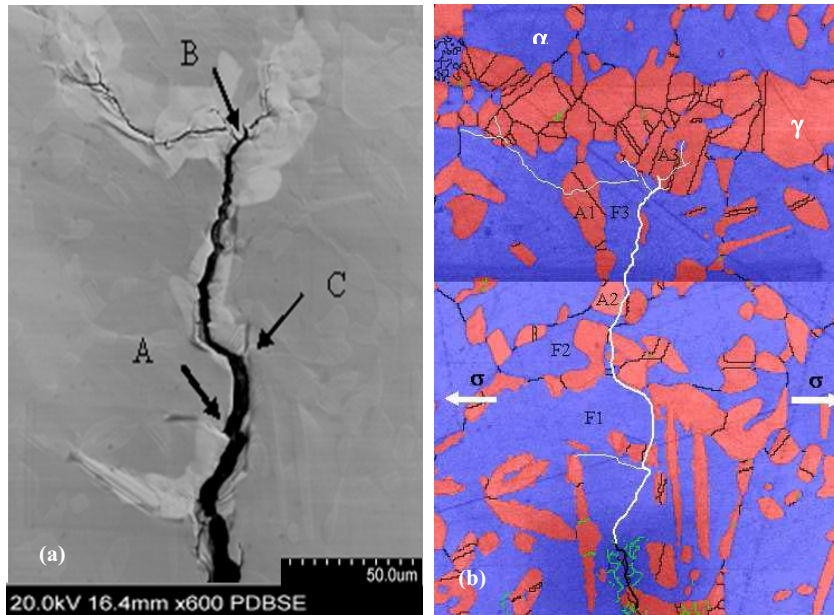


Fig. 5 (a). Backscatter electron image taken after the in-situ fatigue test was terminated and unloaded; (b). EBSD image with crack growth path indicated by thick white line (the main crack) and thin white lines (branches). The dark line is the pre-grown crack by bending fatigue. The loading direction is horizontal.

Table 3 Active slip systems in the ferritic phase

Grain number	[uvw]//LD	Slip system	Schmidt's factor	Slip trace to LD
F1	1-10	$(-112)[1-11]$	0.47	$49^{\circ}/131^{\circ}$
		$(1-12)[-111]$	0.47	$130^{\circ}/50^{\circ}$
F3	22-1	$(11-2)[111]$	0.46	$98^{\circ}/82^{\circ}$
		$(01-1)[111]$	0.41	$128^{\circ}/52^{\circ}$

LD: Loading direction

The fatigue crack path is also indicated in Fig. 5b. The main crack, marked with thick white line, grew from the pre-grown crack (thick black line). Obviously, the observed branching and deflection behavior is dependent on the microstructure. Within the ferritic grains, the crack propagates in a transgranular manner. In the austenitic grains both intergranular and transgranular cracking is observed. A local change of the microstructure, namely the existence of an austenite dominant region in the front of the crack tip causes a large deflection, see for example C in Fig. 5a, or branching (A and B). A closer observation reveals extensive plastic deformation ahead of the crack tip (Fig. 6a), which is evident by dense slip lines found around the crack tip. The delaminated and cracked surface film has prevented the examination of plastic deformation behavior in certain regions. Nevertheless, for transgranular cracking in the ferrite, for which the development of slip lines is clearly visible during the in-situ test, slip on multiple systems is dominant. For example, in the F1 grain two groups of slip bands, determined from the EBSD data to form on the $(-112)[1-11]$ and $(1-12)[-111]$ system (Table 3), respectively, are observed at the crack tip. Both slip systems have a comparable Schmidt's factor of 0.47 but operate in different directions. Extrusions and intrusions develop under repeated cyclic load, the growth of which results in the advance of the crack tip. As Fig. 6b shows, the development of extrusion and intrusion also leads to crack branching in ferritic

grain F3. In the austenite dominant regions, the crack has the tendency to propagate near grain or phase boundaries. One reason could be that local microstresses due to mechanical mismatch between grains or phases [10] could be larger in these regions and they facilitate crack advancing by providing additional driving force.

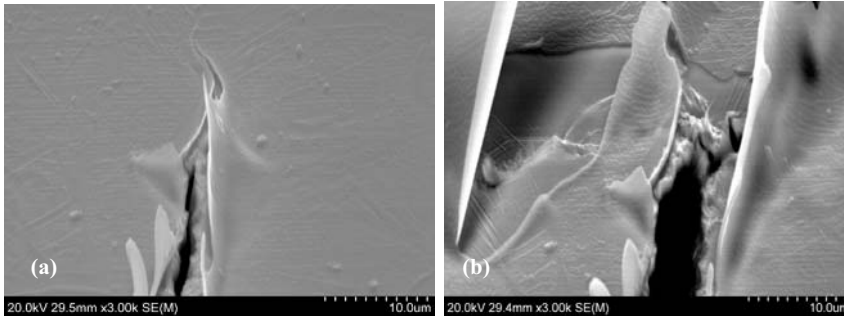


Fig. 6 Crack tip at N=3100 (a) and N=5100 (b) under peak stress.

The main crack length is plotted as a function of the number of loading cycles in Fig. 7a. The average crack propagation rates between two measure points are shown in Fig. 7b. As can be seen the crack growth rate changes at 500 cycles or 3800 cycles (regions A or B) and becomes lower (Fig. 7b). This seems to be connected to the crack branching behavior since the formation of crack branches will reduce the mode I crack driving force, which lead to a crack growth retardation for the main crack path [2-4]. On the other hand, the crack branches grow almost transversely to the main crack direction with a mode II SIF. In the beginning, they propagate with a rate that is much higher than that of the main crack (Fig. 7b), and then the growth will stop somewhere in spite of that its length is longer than that in the main crack path. This can not be the result expected by the analytical solution [4].

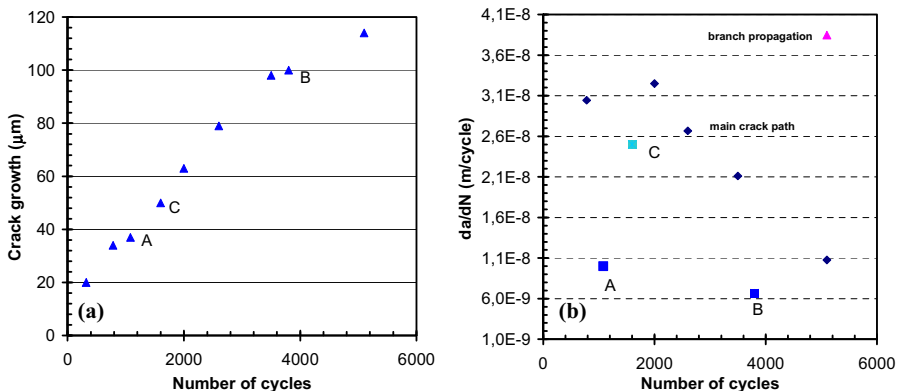


Fig. 7 (a). Crack length versus number of loading cycles; (b). Average crack growth rate versus number of loading cycles, average crack propagation rate was calculated as the ratio of the corresponding loading cycles.

Concluding remarks

Fatigue crack deflection and branching behavior in an UNS S32750 austenitic ferritic duplex stainless steel have been studied using an in-situ SEM/EBSD fatigue test and a conventional da/dN test. The following conclusions have been obtained.

Crack deflection and branching is an important crack propagation behavior in this duplex stainless steel. Crack deflection occurs mainly at the phase boundaries, and crack branching occurs mainly in the grains due to the intrusion and extrusion of the slip bands. The number of crack branches formed depends on the loading condition and the microstructure of the material.

In-situ observation confirms that the formation of crack branches can significantly reduce crack propagation rate that leads to crack growth retardation in the main crack path. The crack branches formed are usually not ideal. They can propagate almost transverse to the main crack direction with a mode II SIF and a rate that is much higher than that of the main crack.

The high crack deflection and branching behavior in the material leads to a high fatigue threshold value since they have caused high crack growth retardation and high crack closure.

Acknowledgment

This paper is published by permission of Sandvik Materials Technology. The support of Prof. O. Wijk and Mr M. Lundström is gratefully acknowledged.

References

- [1] J. Lankford and D.L. Davidson: *Advances in Fracture Research*, Vol. 2 (1981), p. 899.
- [2] S. Suresh: *Engrg Fracture Mechanics*, Vol. 18 (1983), p. 577.
- [3] M.A. Meggiolaro, A.C.O. Miranda, J.T.P. Castro, L.F. Martha: *International Journal of Fatigue* Vol. 27 (2005), p.1398.
- [4] S. Suresh: *Metall Trans*, Vol. 14a (1983), p. 2375.
- [5] A. Akhmad Korda, Y. Mutoh, Y. Miyashita, T. Sadasue, S.L. Mannan: *Scripta Materialia*. Vol. 54, no. 11, (2006), p.1835
- [6] A. Sugeta, Y. Uematsu, E.I. Kuronaga, M. Jono: *Journal of the Society of Materials Science, Japan*, Vol. 54, no. 12, (2005), p. 1268.
- [7] J.K. Shang, J.L. Tzou and R.O. Ritchie: *Metall. Trans. A*, Vol. 18A, (1987), p.1613.
- [8] G. Chai and J. Pokluda: *In: "Fatigue 06"*, Ed. W. S. Johnson, Elsevier, Atlanta, Georgia, USA, p. 0205A_06.
- [9] R. Lillbacka, G. Chai, M. Ekh, P. Liu, E. Johnson, K. Runesson: *Acta Materialia*, Vol. 55 (2007), p. 5359.
- [10] R. Lin Peng, Y.D. Wang, G.C. Chai, N. Jia, S. Johansson, G. Wang: *Materials Science Forum*, v 524-525, 2006, p. 917.